Mathematical Biosciences 387 (2025) 109503

Contents lists available at ScienceDirect

Mathematical Biosciences

journal homepage: www.elsevier.com/locate/mbs

Original research article

Dynamics of bovine tuberculosis transmission in mixed herds in Chad

H. Djimramadji [a], Julien Arino [b,*], P.M. Tchepmo Djomegni [c], M.S. Daoussa Haggar [a]

[a] Department of Mathematics, University of N'Djamena, N'Djamena, Chad
[b] Department of Mathematics, University of Manitoba, Winnipeg, Manitoba, Canada
[c] School of Mathematics and Statistical Sciences, North-West University, South Africa

ARTICLE INFO

Keywords:
Competition model
Bovine tuberculosis
Herd

ABSTRACT

We consider a model for the spread of bovine tuberculosis in herds comprising three species (bovids, caprids and equids) in Chad. The epidemiological model is built on top of a classic Lotka–Volterra competition model, which is exploited in a regime where stable coexistence of the three species holds. The epidemiological model itself is an SLI model, because of the absence of treatment for herds in the area. After studying some mathematical properties of the model, we perform a short computational analysis, investigating sensitivity of the model and comparing solutions with and without competition. To gain more understanding on the timing of events, we also consider the continuous time Markov chain analogue of the model.

1. Introduction

Located in the heart of the African continent, Chad is a landlocked country with a surface area of 1,284,000 square kilometres. The country has an intertropical climate subdivided into three major climatic zones: the Sudanian zone in the south, the Sahelian zone in the centre and the desert zone in the north. As a developing country, Chad's economy is mainly based on agriculture, livestock farming, fishing, gathering, trade and oil and mineral resources.

Due to its geographic location, Chad has a vast territory untouched by the tsetse fly, making it an excellent livestock country. It is estimated that in 2019, livestock production was of more than 120 million animals (32% goats, 29% sheep, 26% cattle and the remaining 13% split between camels, donkeys, horses and pigs) [1]. Over 40% of the population depends on livestock [2]. These figures make Chad one of the major livestock countries in Africa and animal husbandry a crucial sector of the national economy contributing to 40% of the national GDP and playing a major role in food supply [3]. The vastness of Chad's territory and the climatic hazards it faces means that livestock farming in Chad relies on pastoral nomadism, which concerns 90% of Chadian livestock [2]. Inter-seasonal transhumance and the mobility of livestock in search of pasture and water points can affect both animal health and that of the herders. This has been further influenced in recent years by climate change [4].

However, Chad is also a *low-income country* to use the World Bank classification or a *least-developed country* to use the United Nations classification. Its gross national income (GNI) *per capita* is estimated by the World Bank to be 670 USD, the 11th lowest in the world. The country's gross domestic product (GDP) was 13.15 billion USD in 2023, roughly comparable to that of the metropolitan area of the German city of Pforzheim despite a population almost 100 times larger. When considering poor countries, it is important to remember that while the cost of labour roughly scales to *per capita* GDP, the price of imported goods is essentially the same as it is the world over since prices are set by the exporters. As a consequence, public health and animal health control organisms are poorly equipped, meaning that disease surveillance and control lag behind the standards in place in richer countries.

Despite limitations in its capacity, in 2020 the epidemiological surveillance network for animal diseases in Chad (REPIMAT), through the Ministry of Livestock and Animal Production, was monitoring fifteen diseases, including four zoonotic diseases: Bacterial Anthrax, Rift Valley Fever, rabies and bovine Tuberculosis, the focus of the present work. In Chad, bovine tuberculosis is present in livestock, including cattle, sheep, goats, pigs, equids and camelids. Numerous studies conducted across the country have shown that Chad is severely affected by bovine tuberculosis; for instance, out of a sample of 729 animals, bovine tuberculosis accounted for 14% [5]. Similarly, research conducted in some cities in Chad in 2013 showed that in slaughterhouses, there were 332 carcasses of suspected bovine tuberculosis in cattle and 5 carcasses in goats [6]. These various studies lead to estimates of the actual infection rate due to bovine tuberculosis of 12.5% among animals in Chad [6].

Bovine tuberculosis (bTB) is a chronic bacterial disease caused by members of the *Mycobacterium tuberculosis* (*M. bovis*) complex and exists

* Corresponding author.
E-mail address: julien.arino@umanitoba.ca (J. Arino).

https://doi.org/10.1016/j.mbs.2025.109503
Received 2 January 2025; Received in revised form 20 April 2025; Accepted 24 June 2025
Available online 7 July 2025

in both domestic and non-domestic animals. Many mathematical models have been formulated to study the dynamics of bovine tuberculosis in wild animal populations such as buffaloes [7], badgers [8,9], possums [10] and domestic animal populations such as cattle [7,11–15]. However, most of the models cited here use stochastic or agent-based approaches and almost none investigate the transmission of tuberculosis in mixed herds. Competition models with an epidemiological component have also been considered; see, e.g., [16,17]. However, they focus on problems such as pathogen-mediated species coexistence.

Our work aims to improve the understanding of the transmission of bovine tuberculosis infection in places where nomadic managed mixed herds are the most prevalent. On the demographical side, management of herds changes the dynamics quite a lot, since a lot of inflow into and outflow from the herd is due to purchase or sale of animals, not only from natural birth and death processes. Also, even in a managed herd, the scarcity of environmental and financial resources makes competitive pressure within and between species a relevant issue. We however assume that species coexistence holds. Indeed, in managed herds, the population and its composition is roughly constant, with animals being purchased to replace those who leave the herd for any reason. Extending to the epidemiological context, the question underlying the work concerns whether the situation is made better or worse because of the presence of several species, each of which can serve as a reservoir of the disease, as well as by the presence of competition, which could cause shorter survival times for infectious animals.

In order to consider these issues, we formulate in Section 2 a mathematical model for the transmission of bovine tuberculosis infection in a managed mixed herd subject to intra– and interspecific competition. We analyse the model mathematically in Section 3. In Section 4, we make computational considerations about the model, including using a continuous-time Markov chain analogue to check the demographic dynamics and gain a bit more understanding of the transmission process. A Discussion concludes the work.

2. The mathematical model

We consider a model of bovine tuberculosis (bTB) transmission for a farming system comprising bovids, caprids and equids. The three species picked here are representative of herds in the northern Soudanian and Sahelian regions of Chad. Other combinations would have been possible, with for instance camelids replacing equids in the more arid regions in the north of the country [18] or ovines (sheep) replacing bovids in the south. When camelids are present, herd composition with camelids instead of equines is similar to that used here [18]. Also, note that bovids are more varied than what is observed in richer countries; they comprise 4 major species in Chad. Note also that we group together horses and donkeys under the name *equids*. Some herds in Chad comprise more species; others comprise fewer, although single-species herds are much less frequent than they are in richer countries. Altogether, herd composition could differ from the one here: there is much more variety in herds in Chad than there is in the "rationalised" herds of rich countries, probably because having a varied herd allows to edge one's bets in the face of uncertain and difficult conditions.

Whatever the species composing the herd, they are in competition for grazing pastures and water sources, therefore the model incorporates competition. However, the species are managed by the nomadic herding group, who generally ensures their herd comprises the desired number of heads of the species they tend to. Animals are bought to achieve this. Animals are also sold as part of the normal activity of the herders. Finally, all the species considered here as well as potential substitutes (camelids, ovines) are subject to infection by bTB [5,19].

In the following, we start by formulating the model for demography in the absence of disease, then add on the disease component.

2.1. The underlying competition model

Denote $N_b(t)$, $N_c(t)$ and $N_e(t)$ the total bovid, caprid and equid populations, respectively. In the remainder of the text, time dependence of the state variables is omitted if it does not lead to confusion, so the variables above are written N_b, N_c and N_e.

In the absence of disease, we assume that the dynamics of the three interacting species is governed by a classic Lotka–Volterra competition model of the form

$$\frac{d}{dt}N_b = (r_b - d_b)N_b - (d_{bb}N_b + d_{bc}N_c + d_{be}N_e)N_b \tag{2.1a}$$

$$\frac{d}{dt}N_c = (r_c - d_c)N_c - (d_{cb}N_b + d_{cc}N_c + d_{ce}N_e)N_c \tag{2.1b}$$

$$\frac{d}{dt}N_e = (r_e - d_e)N_e - (d_{eb}N_b + d_{ec}N_c + d_{ee}N_e)N_e, \tag{2.1c}$$

where, for species $x \in \{b, c, e\}$, r_x is the *per capita* recruitment rate, d_x is the *per capita* natural death rate and d_{xy} is the rate of death of individuals in species x because of competitive interactions with individuals from species $y \in \{b, c, e\}$. It is always assumed that $r_x - d_x > 0$. We denote $\boldsymbol{N} = (N_b, N_c, N_e)$ the distribution of individuals of the different species in the herd.

Note that in a managed herd, recruitment incorporates birth of individuals as well as acquisition of new individuals to replace the ones sold (e.g., for meat) or having died. Similarly, death incorporates "regular deaths" (whether natural or because of competition) as well as sales of individuals. To simplify the discourse, unless specifically required, we refer to entries into the model as recruitment and all causes of leaving the herd as removal. We will then distinguish between removals because of natural death or sales and because of (intra- or inter-specific) competition.

Remark also that we allow that $d_{xy} \neq d_{yx}$. This is because although the number of contacts happening per unit time between two species is symmetric, the resulting effect on both species might differ.

2.2. The epidemiological model with competition

To describe the progression of bTB, we subdivide compartments N_b, N_c and N_e of individuals in each species into compartments describing the disease status of individuals, while ensuring that the total population in each species is, roughly, governed by (2.1). For a given species $x \in \{b, c, e\}$, we consider the numbers S_x, L_x and I_x of individuals susceptible to, infected with but incubating and infectious with the disease, respectively. We do not consider treatment and therefore recovery of infectious individuals: recommendations in most countries (including Chad) is for animals in which bTB is detected to be culled. Also, the literature indicates that infectious individuals rarely show symptoms until they die from the disease or are detected. As a consequence, we do not consider a recovered compartment R_x.

Let us now explain the assumptions made regarding transitions into or out from the different compartments. First of all, we denote S_x the number of individuals of species x susceptible to infection by bovine tuberculosis. In the absence of disease, this compartment would correspond to the compartment N_x in the competition model (2.1). Recruitment is into this compartment exclusively at the same recruitment rate r_x as used in (2.1). Although vertical transmission of bTB does occur, we neglect it because it is very rare: in [19], it is noted that only 1% of calves born from tuberculous cows were congenitally affected at a time when bTB was highly prevalent. Also, recruitment accounts for both birth and purchase of animals, so that only a fraction of recruitments are "real" births. Similarly, we assume that infected individuals contribute to the overall birth rate. Indeed, as noted already, infectious individuals rarely show symptoms. This is further confirmed implicitly by the statement above that most births from infected cows did not lead to vertical transmission. It could be that some of the animals purchased into the herd are infected. We assume that this is not the case. From an analysis point of view, allowing an

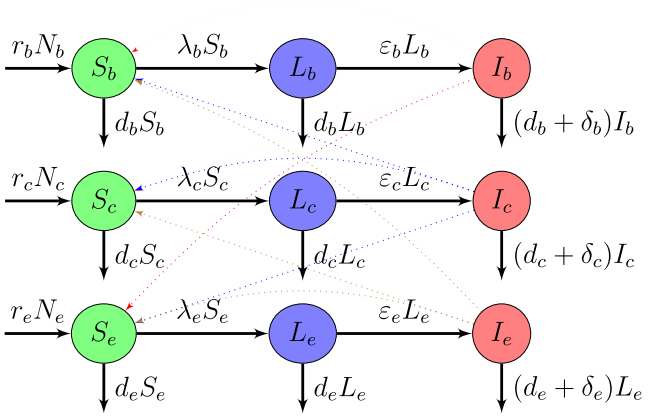

Fig. 1. Flow diagram of model (2.2). Death rates due to competition are not shown.

inflow of infected individuals radically changes the dynamics, given that such models do not have disease-free equilibria; see, e.g., [20]. While it is desirable to further explore this type of dynamics, we do not do so here. From a modelling point of view, this assumption can be justified by the fact that at the moment of a sale, the health of animals is checked.

Transmission happens within and between species, when a susceptible individual in compartment S_x encounters an individual in compartment I_y infectious with the disease, where $x, y \in \{b, c, e\}$ may be equal. We denote β_{xy} the rate of transmission of bTB to a susceptible in species x from an infectious in species y. There are many routes of transmission of bTB, both between and within species: excreta, feeding troughs, soil and silage, herbage, drinking water, etc [19]. This means in particular that direct cross-species transmission between species that show some aversion or hostility is possible through indirect methods. We group all transmission methods together: our focus is not in identifying, for instance, which infection pathway to target in an intervention.

The incubation period of bovine tuberculosis after contamination lasts several months or more [21], so taking this period into account is important. Because clinical symptoms manifest late, if at all, we assume that the latency period is equal to the incubation period. We denote L_x the number of individuals in this incubation period. Upon infection, susceptible individuals thus transition from S_x to L_x. They spend an (exponentially distributed) mean time $1/\varepsilon_x$ time units in that compartment before their incubation period ends and they progress to the infectious compartment. In the infectious compartment, individuals are subject to disease-induced death, which occurs at the *per capita* rate δ_x. Note that this rate also encodes culling, which is the recommended "treatment" mechanism [22]. However, we do not distinguish between disease-induced death and culling as very little data is available on the subject in Chad.

Let us now consider removal terms. Individuals in all compartments are subject to removal because of natural death and sale at the rate d_x. We use the same notation as in (2.1): d_{xy} is the death rate of individuals of species x because of competition with individuals of species y.

The model has the flow diagram shown Fig. 1 and takes the form

$$\frac{dS_b}{dt} = r_bN_b - (\lambda_b + d_b)S_b - (d_{bb}N_b + d_{bc}N_c + d_{be}N_e)S_b \tag{2.2a}$$
$$\frac{dL_b}{dt} = \lambda_bS_b - (\varepsilon_b + d_b)L_b - (d_{bb}N_b + d_{bc}N_c + d_{be}N_e)L_b \tag{2.2b}$$
$$\frac{dI_b}{dt} = \varepsilon_bL_b - (\delta_b + d_b)I_b - (d_{bb}N_b + d_{bc}N_c + d_{be}N_e)I_b \tag{2.2c}$$
$$\frac{dS_c}{dt} = r_cN_c - (\lambda_c + d_c)S_c - (d_{cb}N_b + d_{cc}N_c + d_{ce}N_e)S_c \tag{2.2d}$$
$$\frac{dL_c}{dt} = \lambda_cS_c - (\varepsilon_c + d_c)L_c - (d_{cb}N_b + d_{cc}N_c + d_{ce}N_e)L_c \tag{2.2e}$$
$$\frac{dI_c}{dt} = \varepsilon_cL_c - (\delta_c + d_c)I_c - (d_{cb}N_b + d_{cc}N_c + d_{ce}N_e)I_c \tag{2.2f}$$
$$\frac{dS_e}{dt} = r_eN_e - (\lambda_e + d_e)S_e - (d_{eb}N_b + d_{ec}N_c + d_{ee}N_e)S_e \tag{2.2g}$$
$$\frac{dL_e}{dt} = \lambda_eS_e - (\varepsilon_e + d_e)L_e - (d_{eb}N_b + d_{ec}N_c + d_{ee}N_e)L_e \tag{2.2h}$$
$$\frac{dI_e}{dt} = \varepsilon_eL_e - (\delta_e + d_e)I_e - (d_{eb}N_b + d_{ec}N_c + d_{ee}N_e)I_e, \tag{2.2i}$$

where, for species $x \in \{b, c, e\}$, $N_x = S_x + L_x + I_x$ is the total population of the species and

$$\lambda_x = \beta_{xb}I_b + \beta_{xc}I_c + \beta_{xe}I_e \tag{2.3}$$

is the force of infection acting on susceptibles from species x.

For convenience, in the sequel, for $t \geq 0$, we denote

$$\mathbf{X}(t) = (S_b(t), S_c(t), S_e(t), L_b(t), L_c(t), L_e(t), I_b(t), I_c(t), I_e(t))^T \tag{2.4}$$

the vector of state variables, in which variables are ordered first by disease status, then by species. System (2.2) is considered together with the initial condition

$$\mathbf{X}(0) \geq \mathbf{0}. \tag{2.5}$$

3. Mathematical analysis of the model

We first recall in Section 3.1 a result obtained in [23] that establishes conditions under which (2.1) converges to a coexistence equilibrium. We then consider in Section 3.2 the model in which species do not interact, allowing the derivation of a species-specific basic reproduction number. Assuming that conditions for the stable coexistence of the three species are satisfied, we then consider the full epidemiological model (2.2) in Section 3.3.

3.1. *The underlying competition model* (2.1)

The three-dimensional Lotka–Volterra competition system (2.1) has been investigated mathematically for years; see for instance [24] for a brief review. In short, in the three-dimensional case, it is known since [25] that all nontrivial trajectories of (2.1) approach a Lipchitz two-dimensional manifold-with-corner Σ homeomorphic to the standard simplex in $\mathbb{R}^3_+$, which [25] called the "carrying simplex". Building on this, [26] showed that there are 33 equivalence classes as to the dynamics of the system, with most 27 having solutions converging to equilibrium points, while the remaining can show limit cycles. Most of mathematical work that followed has focused on limit cycles; for examples, besides the works already cited see, e.g., [27–29].

We are interested here in a "simpler" coexistence situation, since in practice, in a managed herd the three species are present at relatively constant levels. Oscillatory coexistence could be a viable option, but this would greatly complicate the mathematical analysis of the epidemiological model. Also, because the situation is managed, one does not observe great variations in abundances: animals that die because of competition for resources are replaced by the herders in order to maintain a relatively stable herd size and composition. This suggests that a non-oscillatory coexistence situation is more likely. As a consequence, we seek to use the system in parameter ranges where [23, Corollary 1.4] holds true, i.e., where solutions converge to a positive equilibrium.

Note that (2.1) is formulated in [23] using $a_{ij} = d_{ij}$ and $b_i = r_i - d_i$. The analysis in [23] is directly applicable here; we briefly summarise it below in terms of the parameters used in [23] and interpret it in view of our specific use case. Refer to [23,25,26] for details about the mathematical analysis.

Regarding equilibria, first observe that the origin is an unstable equilibrium of (2.1), since the Jacobian matrix there is $\mathrm{diag}(r_b - d_b, r_c - d_c, r_e - d_e)$, with all these terms positive by assumption. Note, then, as in [23], that the basin of repulsion of the origin in $\mathbb{R}^3_+$ is bounded. Call

carrying simplex of (2.1) and denote Σ the boundary of that basin. Σ is a surface in $\mathbb{R}^3_+$ such that each trajectory of (2.1) is asymptotic to one in Σ. Following [25,26], one can study (2.1) on Σ.

On each axis of $\mathbb{R}^3_+$, (2.1) reduces to the logistic equation $N_x' = (r_x - d_x)N_x - d_{xx}N_x^2$, $x \in \{b,c,e\}$. Denote $N_x^\star$, $x \in \{b,c,e\}$, the equilibria of these equations on the N_x axes, i.e., $N_x^\star = (r_x - d_x)/d_{xx} > 0$. Let $\boldsymbol{R}_b^\star = (N_b^\star, 0, 0)$, $\boldsymbol{R}_c^\star = (0, N_c^\star, 0)$ and $\boldsymbol{R}_e^\star = (0, 0, N_e^\star)$ be the corresponding boundary equilibria. All these equilibria are in Σ.

Additionally to these single species boundary equilibria, there are, as noted in Section 2.3 of [26], three boundary equilibria in Σ with two species present. Finally, there is potentially an interior equilibrium with the three species present,

$$\boldsymbol{P}^\star = (P_b^\star, P_c^\star, P_e^\star), \tag{3.6}$$

with components taking the form

$$P_b^\star = \frac{\left(d_{cc}d_{ee} - d_{ce}d_{ec}\right)d_{bb}N_b^\star + \left(d_{be}d_{ec} - d_{bc}d_{ee}\right)d_{cc}N_c^\star + \left(d_{bc}d_{ce} - d_{be}d_{cc}\right)d_{ee}N_e^\star}{\left(d_{bb}d_{cc} - d_{bc}d_{cb}\right)d_{ee} + \left(d_{be}d_{cb} - d_{bb}d_{ce}\right)d_{ec} + \left(d_{bc}d_{ce} - d_{be}d_{cc}\right)d_{eb}},$$

$$P_c^\star = \frac{\left(d_{ce}d_{eb} - d_{cb}d_{ee}\right)d_{bb}N_b^\star + \left(d_{bb}d_{ee} - d_{be}d_{eb}\right)d_{cc}N_c^\star + \left(d_{be}d_{cb} - d_{bb}d_{ce}\right)d_{ee}N_e^\star}{\left(d_{bb}d_{cc} - d_{bc}d_{cb}\right)d_{ee} + \left(d_{be}d_{cb} - d_{bb}d_{ce}\right)d_{ec} + \left(d_{bc}d_{ce} - d_{be}d_{cc}\right)d_{eb}},$$

$$P_e^\star = \frac{\left(d_{cb}d_{ec} - d_{cc}d_{eb}\right)d_{bb}N_b^\star + \left(d_{bc}d_{eb} - d_{bb}d_{ec}\right)d_{cc}N_c^\star + \left(d_{bb}d_{cc} - d_{bc}d_{cb}\right)d_{ee}N_e^\star}{\left(d_{bb}d_{cc} - d_{bc}d_{cb}\right)d_{ee} + \left(d_{be}d_{cb} - d_{bb}d_{ce}\right)d_{ec} + \left(d_{bc}d_{ce} - d_{be}d_{cc}\right)d_{eb}}.$$

When that equilibrium is biologically relevant, the following result established as Corollary 1.4 in [23] then holds.

Theorem 1 ([23]). *Suppose that for $x, y \in \{b,c,e\}$, $y \neq x$, $r_x - d_x, d_{xy} > 0$,*

$$d_{xy} < \frac{r_x - d_x}{N_y^\star} \tag{3.7}$$

and that there exists $\boldsymbol{P}^\star = (P_b^\star, P_c^\star, P_e^\star) \in \Sigma$ in the interior of $\mathbb{R}^3_+$. Then $\boldsymbol{P}^\star$ is globally asymptotically stable in $\mathrm{int}(\mathbb{R}^3_+)$.

The proof can be found in [23] and is therefore not reproduced here. However, let us briefly detail the specific expressions found in Theorem 1. The Jacobian matrix of (2.1) at $\boldsymbol{R}_x^\star$, $x \in \{b,c,e\}$, has eigenvalues $-(r_x - d_x) < 0$ and

$$r_y - d_y - d_{yx}N_x^\star, \quad y \in \{b,c,e\}, \quad y \neq x.$$

Thus, the local asymptotic stability of $\boldsymbol{R}_x^\star$ depends on the sign of the latter two eigenvalues, with $\boldsymbol{R}_x^\star$ a repeller (a condition of [23, Corollary 1.4]) if both are positive. The carrying capacities $N_x^\star = (r_x - d_x)/d_{xx}$ for the different species can be assumed known, so we express the conditions in terms of interspecific competition rates, giving condition (3.7).

Establishing that (3.6) is strongly positive under the other conditions of Theorem 1 is not trivial analytically. However, the computational method detailed in Section 4.1 allows to establish that there are indeed points in parameter space where $\boldsymbol{P}^\star \gg \boldsymbol{0}$, i.e., where Theorem 1 applies. Note that it is also easy to establish that $\boldsymbol{P}^\star \ll (N_b^\star, N_c^\star, N_e^\star)$, which greatly helps when seeking parameter values in Section 4.1.

3.2. The epidemiological model for an isolated species

In the case where species do not interact with each other, i.e., $d_{xy} = \beta_{xy} = 0$ whenever $x \neq y$, the model for species $x \in \{b,c,e\}$ takes the form

$$\frac{d}{dt}S_x = r_xN_x - (\beta_{xx}I_x + d_x)S_x - d_{xx}N_xS_x \tag{3.8a}$$

$$\frac{d}{dt}L_x = \beta_{xx}S_xI_x - (\varepsilon_x + d_x)L_x - d_{xx}N_xL_x \tag{3.8b}$$

$$\frac{d}{dt}I_x = \varepsilon_xL_x - (\delta_x + d_x)I_x - d_{xx}N_xI_x. \tag{3.8c}$$

Thus, the single species model (3.8) has logistic type dynamics, with total population governed by

$$\frac{d}{dt}N_x = (r_x - d_x)N_x - d_{xx}N_x^2 - \delta_xI_x(t), \tag{3.9}$$

where $I_x(t)$ is given by (3.8c), but can also be considered as a time-dependent C^1 function such that $I_x(t) \in [0, N_x^\star]$ for all sufficiently large $t \in \mathbb{R}_+$. Actually, $I_x(t) \in [0, N_x(t))$, where $N_x(t) = S_x(t) + L_x(t) + I_x(t)$ is computed from the solutions of (3.8), but in practice, since $I_x(t) \geq 0$ for all $t \geq 0$, $I_x(t)$ is bounded above by the solution of (3.9) from which the term δ_xI_x has been removed, i.e., a classic logistic equation.

At the disease-free equilibrium, $S_x = N_x$ and (3.8) reduces to the single equation

$$\frac{d}{dt}S_x = r_xS_x - d_xS_x - d_{xx}S_x^2.$$

This is a classic logistic equation, with all positive S_x solutions tending to the single-species carrying capacity $N_x^\star = (r_x - d_x)/d_{xx}$. (We exclude the zero solution, which is of no interest.) Therefore, the disease-free equilibrium point of (3.8) is

$$\boldsymbol{E}_0^{x\star} = \left(N_x^\star, 0, 0\right). \tag{3.10}$$

Using the method of [30], we set

$$\mathcal{F} = \begin{pmatrix} \beta_{xx}S_xI_x \\ 0 \end{pmatrix}$$

and

$$\mathcal{V} = \begin{pmatrix} (\varepsilon_x + d_x + d_{xx}N_x)L_x \\ -\varepsilon_xL_x + (\delta_x + d_x + d_{xx}N_x)I_x \end{pmatrix}.$$

Therefore,

$$F = \begin{pmatrix} 0 & \beta_{xx}N_x^\star \\ 0 & 0 \end{pmatrix}$$

and, writing $N_x = S_x + L_x + I_x$, differentiating $\mathcal{V}$ with respect to L_x and I_x and setting them equal to zero and $S_x = N_x^\star$,

$$V = \begin{pmatrix} \varepsilon_x + d_x + d_{xx}N_x^\star & 0 \\ -\varepsilon_x & \delta_x + d_x + d_{xx}N_x^\star \end{pmatrix}.$$

It follows that the basic reproduction number for species x in isolation is

$$\mathcal{R}_0^x = \frac{\varepsilon_x\beta_{xx}N_x^\star}{(\varepsilon_x + d_x + d_{xx}N_x^\star)(\delta_x + d_x + d_{xx}N_x^\star)}. \tag{3.11}$$

Note that it is possible to obtain a simpler expression by using the fact that, e.g., the (1,1) term in V can also be written as $\varepsilon_x + d_x + d_{xx}N_x^\star = r_x + \varepsilon_x$. However, there are situations in the computational analysis where we wish to "hide" the role of r_x, so we use the form above.

From [30, Theorem 2], we get the following result.

Lemma 2. *Suppose that there are no interactions between species, so that for $x \in \{b,c,e\}$, (2.2) reduces to (3.8). Then, if for species $x \in \{b,c,e\}$, $\mathcal{R}_0^x < 1$, where $\mathcal{R}_0^x$ is defined by (3.11), then the disease-free equilibrium (3.10) for species x is locally asymptotically stable. If $\mathcal{R}_0^x > 1$, it is unstable.*

It is easy to show that the result is actually global when $\mathcal{R}_0^x < 1$, but our main use for Lemma 2 lies in the computation of $\mathcal{R}_0^x$, which is useful later in the computational analysis, so we forgo this here.

Let us say a word here about endemic equilibria, since the issue that arises is also present even more acutely in the full model (2.2). The problem is more complicated than the disease-free case. Indeed, while at the DFE, we have $S_x = N_x$ for all species $x \in \{b,c,e\}$, the same is not true when disease is present. Computing endemic equilibria then involves using (3.8) with $N_x = S_x + L_x + I_x$, since in (3.9), the term δ_xI_x does not vanish. This means that instead of having a single nonlinearity $\beta_{xx}S_xI_x$ to deal with, there are ten, since terms $d_{xx}(S_x + L_x + I_x)S_x$, $d_{xx}(S_x + L_x + I_x)L_x$ and $d_{xx}(S_x + L_x + I_x)I_x$ are also present.

We suspect and numerical work strongly suggests that (3.8) has a single endemic equilibrium point that is globally asymptotically stable when $\mathcal{R}_0 > 1$

3.3. The full epidemiological model

Here, we suppose that Theorem 1 holds true, i.e., that the underlying demographic model with competition converges to the globally asymptotically stable equilibrium point $\boldsymbol{P}^\star$ given by (3.6).

First, note that the right hand side of (2.2) is C^1, so solutions to (2.2) exist and are unique. It is also easy to show that the positive orthant is invariant under the flow of (2.2) and furthermore, that all solutions of (2.2) with initial number of individuals in all species $N_x(0) = S_x(0)+L_x(0)+I_x(0) > 0$ eventually enter the positively invariant set

$$\Omega_D = \left\{\mathbf{X} \in \mathbb{R}^9; 0 < S_x + L_x + I_x \le N_x^\star \text{ for } x \in \{b,c,e\}\right\}, \tag{3.12}$$

where $N_b^\star$, $N_c^\star$ and $N_e^\star$ are the nonzero components of the boundary equilibria $\boldsymbol{N}_b^\star$, $\boldsymbol{N}_c^\star$ and $\boldsymbol{N}_e^\star$ of (2.1), respectively.

3.3.1. The disease-free equilibrium

One important observation follows, whose proof is omitted because it is trivial.

Lemma 3. *The set*

$$\Gamma = \left\{\mathbf{X}(t) \in \mathbb{R}^9_+;\ L_b = L_c = L_e = I_b = I_c = I_e = 0\right\} \tag{3.13}$$

is positively invariant under the flow of (2.2). On that set, (2.2) reduces to (2.1).

This means that the disease free equilibrium has all $L_x = I_x = 0$ and $(S_b, S_c, S_e) = (P_b^\star, P_c^\star, P_e^\star)$, where $\boldsymbol{P}^\star = (P_b^\star, P_c^\star, P_e^\star)$ is the coexistence equilibrium of (2.1) whose existence is a conclusion of Theorem 1.

In what follows, compartments are ordered first by disease status, then by species. The disease-free equilibrium point is thus given by

$$\boldsymbol{E}_0^\star = \left(P_b^\star, P_c^\star, P_e^\star, 0, 0, 0, 0, 0, 0\right). \tag{3.14}$$

Another important consequence of Lemma 3 is that although it is not possible to establish convergence of the total population of each species when disease is present, at the disease-free equilibrium we do have $N_x = S_x = P_x^\star$ for $x \in \{b,c,e\}$.

Bear in mind, though, that this value of N_x differs from the boundary equilibria carrying capacities $N_x^\star = (r_x - d_x)/d_{xx}$ discussed in Section 3.1 and used when defining Ω_D in (3.12).

3.3.2. The basic reproduction number

To calculate the reproduction number $\mathcal{R}_0$ of the model, we use the next generation matrix method [30]. Infected compartments are $\mathcal{I} = \left(L_b, L_c, L_e, I_b, I_c, I_e\right)$. We first form the vectors $\mathcal{F}$ and $-\mathcal{V}$ of new infections into $\mathcal{I}$ and flows within and out of $\mathcal{I}$, respectively. We have

$$\mathcal{F} = \begin{pmatrix} \left(\beta_{bb}I_b + \beta_{bc}I_c + \beta_{be}I_e\right)S_b \\ \left(\beta_{cb}I_b + \beta_{cc}I_c + \beta_{ce}I_e\right)S_c \\ \left(\beta_{eb}I_b + \beta_{ec}I_c + \beta_{ee}I_e\right)S_e \\ 0 \\ 0 \\ 0 \end{pmatrix}$$

and

$$\mathcal{V} = \begin{pmatrix} (\varepsilon_b + d_b)L_b + (d_{bb}N_b + d_{bc}N_c + d_{be}N_e)L_b \\ (\varepsilon_c + d_c)L_c + (d_{cb}N_b + d_{cc}N_c + d_{ce}N_e)L_c \\ (\varepsilon_e + d_e)L_e + (d_{eb}N_b + d_{ec}N_c + d_{ee}N_e)L_e \\ -\varepsilon_b L_b + (\delta_b + d_b)I_b + (d_{bb}N_b + d_{bc}N_c + d_{be}N_e)I_b \\ -\varepsilon_c L_c + (\delta_c + d_c)I_c + (d_{cb}N_b + d_{cc}N_c + d_{ce}N_e)I_c \\ -\varepsilon_e L_e + (\delta_e + d_e)I_e + (d_{eb}N_b + d_{ec}N_c + d_{ee}N_e)I_e \end{pmatrix}.$$

Matrix F is obtained by taking the Fréchet derivative $D_{\mathcal{I}}\mathcal{F}$ of $\mathcal{F}$ with respect to $\mathcal{I}$ and evaluating at the disease-free equilibrium. It follows that F is a 2×2 block matrix, with the only nonzero block F_{12} taking the form

$$F_{12} = \begin{pmatrix} \beta_{bb}P_b^\star & \beta_{bc}P_b^\star & \beta_{be}P_b^\star \\ \beta_{cb}P_c^\star & \beta_{cc}P_c^\star & \beta_{ce}P_c^\star \\ \beta_{eb}P_e^\star & \beta_{ec}P_e^\star & \beta_{ee}P_e^\star \end{pmatrix}. \tag{3.15}$$

Because of competition terms, matrix $V = D_{\mathcal{I}}\mathcal{V}(\boldsymbol{E}_0^\star)$ is more complicated. It takes the form

$$V = \begin{pmatrix} V_{11}^O + V_{11}^C & \mathbf{0} \\ V_{21}^O & V_{22}^O + V_{11}^C \end{pmatrix},$$

where

$$V_{11}^O = \mathrm{diag}(\varepsilon_b + d_b, \varepsilon_c + d_c, \varepsilon_e + d_e),$$
$$V_{21}^O = -\mathrm{diag}(\varepsilon_b, \varepsilon_c, \varepsilon_e),$$
$$V_{22}^O = \mathrm{diag}(\delta_b + d_b, \delta_c + d_c, \delta_e + d_e)$$

and

$$V_{11}^C = V_{22}^C = \mathrm{diag}\left(d_{bb}P_b^\star + d_{bc}P_c^\star + d_{be}P_e^\star, d_{cb}P_b^\star + d_{cc}P_c^\star + d_{ce}P_e^\star, d_{eb}P_b^\star + d_{ec}P_c^\star + d_{ee}P_e^\star\right).$$

Because of the structure of F, we have

$$FV^{-1} = \begin{pmatrix} F_{12}V_{21}^{-1} & F_{12}V_{22}^{-1} \\ \mathbf{0} & \mathbf{0} \end{pmatrix},$$

and the basic reproduction number takes the form

$$\mathcal{R}_0 = \rho\left(F_{12}(V_{22}^0 + V_{11}^C)^{-1}\mathrm{diag}(\varepsilon_b, \varepsilon_c, \varepsilon_e)(V_{11}^O + V_{11}^C)^{-1}\right). \tag{3.16}$$

It is straightforward to check that hypotheses A1-A5 in [30, Theorem 2] are satisfied, with in particular A5 (typically, the most difficult to check) stemming from Lemma 3 and Theorem 1. As a consequence, the reasoning above implies that the following result holds true.

Theorem 4. *The disease-free equilibrium $\boldsymbol{E}_0^\star$ is locally asymptotically stable if $\mathcal{R}_0 < 1$ and unstable if $\mathcal{R}_0 > 1$.*

As the nonzero block matrices in (3.16) are all diagonal matrices, the inverses are easily computed, so an explicit expression of $\mathcal{R}_0$ can be obtained. However, this expression is very long (it occupies several pages) and little is gained from making it explicit. Indeed, the only circumstance in the sequel where this expression could be of use is if we computed explicitly the dependence of $\mathcal{R}_0$ on parameters, but even these expressions would be too complicated to make sense of except numerically. Instead, remark that $\mathcal{R}_0$ is easily computed numerically once parameters are set.

3.3.3. Global asymptotic stability of the DFE when $\mathcal{R}_0 < 1$

To show that the disease-free equilibrium is actually globally asymptotically stable when $\mathcal{R}_0 < 1$, let us first establish the following.

Lemma 5. *The set*

$$\Psi = \left\{\mathbf{X} \in \mathbb{R}^9_+;\ 0 < N_x < P_x^\star \text{ for } x \in \{b,c,e\}\right\} \tag{3.17}$$

attracts all solutions of (2.2) having initial conditions with $L_x(0)+I_x(0) > 0$ for all $x \in \{b,c,e\}$. In turn, this means that for all $x \in \{b,c,e\}$, $S_x(t) < P_x^\star$ for all sufficiently large t.

Proof. By the assumption $L_x(0) + I_x(0) > 0$ for all $x \in \{b,c,e\}$, initial conditions are not in the set Γ defined by (3.13). As a consequence, $I_x(t) > 0$ for all $t \in \mathbb{R}_+$ and $x \in \{b,c,e\}$, even if it limits to zero. Under the conditions of Theorem 1, all solutions of (2.1) with positive initial conditions tend to $\boldsymbol{P}^\star$. As a consequence, for $x \in \{b,c,e\}$, at $P_x^\star$, $N_x' = 0$ for (2.1).

Now consider the total population of each species $N_x = S_x + L_x + I_x$ in (2.2). It is governed by

$$N_x' = (r_x - d_x)N_x - d_{xx}N_x^2 - \delta_x I_x,$$

where I_x can either be considered as a time dependent function or as a solution of (2.2). In either case, since $I_x(t) > 0$ for all $t \in \mathbb{R}_+$ and $x \in \{b,c,e\}$, it follows that $N_x' < 0$ at $P_x^\star$ for the epidemiological model. Thus, in the epidemiological model, the total population N_x for species x eventually becomes smaller than $P_x^\star$. The conclusion about S_x then is trivial. □

Theorem 6. *Suppose that initial conditions to (2.2) are such that* $\mathbf{0} \ll \boldsymbol{N}(0) \ll \boldsymbol{P}^\star$ *with* $\boldsymbol{L}(0)+\boldsymbol{I}(0) \gg \mathbf{0}$. *Assume that* $\mathcal{R}_0 < 1$, *with* $\mathcal{R}_0$ *defined by (3.16). Then the disease-free equilibrium (3.14) is globally asymptotically stable.*

Proof. We use results of [31], which involves setting

$$f(x_S, x_I) := (F - V)x_I - \mathcal{F}(x_S, x_I) + \mathcal{V}(x_S, x_I)$$

so that disease compartments x_I can be written as

$$x_I' = (F - V)x_I - f(x_S, x_I).$$

Note that we have slightly changed the notation of [31]. We have

$$f(x_S, x_I) = \begin{pmatrix} (\beta_{bb}I_b + \beta_{bc}I_c + \beta_{be}I_e)(P_b^\star - S_b) \\ (\beta_{cb}I_b + \beta_{cc}I_c + \beta_{ce}I_e)(P_c^\star - S_c) \\ (\beta_{eb}I_b + \beta_{ec}I_c + \beta_{ee}I_e)(P_e^\star - S_e) \\ 0 \\ 0 \\ 0 \end{pmatrix}.$$

From Lemma 5, we have $f(x_S, x_I) \geq 0$ for all sufficiently large t, provided initial conditions are such that $L_x(0) + I_x(0) > 0$ for all $x \in \{b, c, e\}$. That the matrices F and V^{-1} are nonnegative is a direct consequence of their construction and is easy to check in any event.

It then follows from [31, Theorem 2.1] that $Q = \omega^T V^{-1} x_I$ is a Lyapunov function for (2.2) when $\mathcal{R}_0 < 1$, where ω is the left eigenvector of $V^{-1}F$ corresponding to the eigenvalue $\mathcal{R}_0 = \rho(V^{-1}F) = \rho(FV^{-1})$.

It is however not possible to use a result such as [31, Theorem 2.2] to conclude, since the presence of latent compartments implies that the matrix $V^{-1}F$ is reducible. However, we can follow the same procedure as in Section 5 in [31] to conclude that the disease-free equilibrium is globally asymptotically stable in Ψ. □

4. Computational investigation

To complement the mathematical analysis of Section 3, we proceed here to a brief computational investigation of the properties of (2.1) and (2.2). We start by parametrising the competition model through an inverse approach (Section 4.1) and the epidemiological model (Section 4.2). These parameters having been chosen, we conduct a sensitivity analysis of $\mathcal{R}_0$ to system parameters in Section 4.3. In Section 4.4, we consider the effect of competition in the epidemiological model. Finally, in Section 4.5 we extend the computational analysis by considering the continuous-time Markov chain equivalents to (2.1) and (2.2).

4.1. Parametrisation of the competition model

Finding values for parameters relative to species recruitment, removal and competition-induced death requires to consider an inverse problem.

First, we decide on herd composition. In the sequel, we want herds with $\tilde{P}_b^\star = 300$ bovids, $\tilde{P}_c^\star = 200$ caprids and $\tilde{P}_e^\star = 60$ equids. This corresponds to a typical camp herd in Chad [18,32,33]. (Camps comprise several households, each of which has a herd, but these herds are kept together.)

We then seek parameters such that Theorem 1 holds with the equilibrium $\boldsymbol{P}^\star$ given by (3.6) "close" to the desired population composition equilibrium $\tilde{\boldsymbol{P}}^\star = (\tilde{P}_b^\star, \tilde{P}_c^\star, \tilde{P}_e^\star)$. Regarding "closeness", we use a classic least squares, i.e., we minimise

$$e = \sum_{x \in \{b,c,e\}} \left(\tilde{P}_x^\star - P_x^\star\right)^2.$$

We assume that the average durations of life are exponentially distributed with durations of $1/d_b$, $1/d_c$ and $1/d_e$ of 12, 8 and 16 years for bovids, caprids and equids, respectively. (These values are smaller than the "nominal" life expectancy for these species because death rates also include selling an animal out of the herd.) We then seek values of the remaining demographic and competition parameters in a hyperrectangle $\mathcal{H}$ in the interior of $\mathbb{R}_+^{12}$. For each point in $\mathcal{H}$, we further check that they satisfy the constraints in Theorem 1 while giving $\boldsymbol{P}^\star \gg \mathbf{0}$.

Because of the constraints in the search domain, we use a genetic algorithm to minimise e. Specifically, we use the function `gaisl` in the R package `GA` [34] to seek points in $\mathcal{H}$ that maximise $-e$, since genetic algorithms are usually maximisers. Any point in $\mathcal{H}$ that violates one of the constraints is given an infinite error and is therefore ignored.

With the parameters in Table 1, we find the equilibrium $\boldsymbol{P}^\star = (299.99998, 200.00001, 60.00001)$, close to the desired $\tilde{\boldsymbol{P}}^\star$. We use these parameters for the demographic and competition components from now on.

Table 1
Demographic model parameters (including those related to competition) as found by the genetic algorithm.

Symbol	Definition	Value
r_b	Recruitment of bovids	0.0004733018
r_c	Recruitment of caprids	0.0004892810
r_e	Recruitment of equids	0.0004323007
d_b	Natural deaths of bovids	0.0002281542
d_c	Natural deaths of caprids	0.0003422313
d_e	Natural deaths of equids	0.0001711157
d_{bb}	Death of bovids b/c of competition with bovids	5.980337e−07
d_{bc}	Death of bovids b/c of competition with caprids	2.853962e−07
d_{be}	Death of bovids b/c of competition with equids	1.443031e−07
d_{cb}	Death of caprids b/c of competition with bovids	1.998480e−07
d_{cc}	Death of caprids b/c of competition with caprids	4.002224e−07
d_{ce}	Death of caprids b/c of competition with equids	1.175133e−07
d_{eb}	Death of caprids b/c of competition with bovids	4.414511e−07
d_{ec}	Death of caprids b/c of competition with caprids	4.794541e−07
d_{ee}	Death of caprids b/c of competition with equids	5.476484e−07

4.2. Parametrisation of the epidemiological component

To parametrise the epidemiological model, we first collect some information from the literature. Some parameters can be found in papers about existing models such as [7,10,15], but they correspond to very different models to the one here and are therefore not relevant. Regarding bovines, [35] gives some information; see also [36]. In experiments, incubation periods depend on the size of the initial inoculation, ranging from two months in the case of inoculation with a very large dose to no symptoms ever in the case of extremely small inoculations. We therefore consider $1/\varepsilon_b \in [2 \text{ months}; 50 \text{ years}]$, with, when fixed, an average of 2 years. (We set an unrealistically high maximum latency period for the upper bound to ensure the other events affecting latent individuals, i.e., natural deaths, occur before.) We vary $1/\varepsilon_c$ and $1/\varepsilon_e$ in the same range, but when using a set value, use $1/\varepsilon_c$ of 1 year and $1/\varepsilon_e$ of 3 years.

Regarding the rates of disease-induced death δ_x, pinpointing the exact time from infection to death is challenging. The available literature provides limited specific information on this aspect. This is mainly due to the fact that in many countries, a diagnosis of bovine TB leads to culling of the infected animal. This right censorship implies that case-fatality ratio information is equally challenging to find. While there is a push to move towards a less stringent process [37], the data is still absent as yet. For this reason, we use values in the range $1/\delta_x \in [2 \text{ weeks}; 6 \text{ months}]$ and a specific value of $1/\delta_x$ of 1 month.

Parametrising the transmission coefficients β is extremely difficult, so we proceed as follows. We assume a value of $\mathcal{R}_0^x$ for species $x \in \{b, c, e\}$ in isolation, then using (3.11) and other parameters, we deduce the value of β_{xx}. Values for the inter-species transmission coefficients β_{xy}, $x, y \in \{b, c, e\}$, $x \neq y$, are even harder to estimate. We assume that they are somewhat lower than those for transmission between

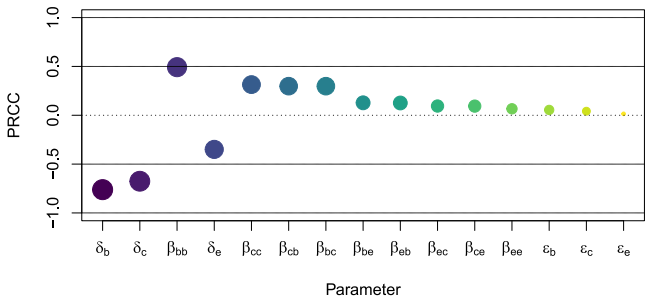

Fig. 2. Sensitivity of $\mathcal{R}_0$ given by (3.16) to changes in the indicated parameters sorted in decreasing order of PRCC magnitude.

individuals of the same species because of potential conflicts between species.

4.3. Sensitivity analysis of $\mathcal{R}_0$

To investigate the effect of the various epidemiological parameters on the system, we proceed to a simple global sensitivity analysis. For this, we choose 500,000 points in parameter space using Sobol sampling through the R library `sensitivity`, compute the value of $\mathcal{R}_0$ as given by (3.16) for each of these points in parameter space, then compute the partial rank correlation coefficients (PRCC). Note that here, values of β_{xy} are all allowed to vary within the range [5e-7,2e−04], which we found below (Fig. 3) to lead to $\mathcal{R}_0$ values in a reasonable range of 0.01 to about 5.5. The result is shown in Fig. 2.

We observe that all parameters except for the disease-induced death rates δ_x have a positive influence on the value of $\mathcal{R}_0$ and that, save for β_{bb}, the most effect on the value of $\mathcal{R}_0$ is due to the disease-induced death rates δ_x. Recall that these rates include (implicitly) the culling rate; so, in view of Fig. 2, culling is indeed a powerful mechanism of disease control. Another observation is that the size of the species population within the herd plays an important role: parameters linked to equids are, generally, less influent than those of the two other species. While expected, this means that if control mechanisms are available, then the largest effect on $\mathcal{R}_0$ is obtained by targetting the largest population. Finally, the average duration $1/\epsilon_x$ of the incubation period has the lowest influence on $\mathcal{R}_0$, regardless of the distribution of individuals from the different species present.

In Fig. 3, we dig further into the relationship between inter-species transmission parameters β_{xy}, $x \neq y$ and the within-species transmission parameters β_{xx}. Using other parameters as described in Sections 4.1 and 4.2, we plot the value of $\mathcal{R}_0$ as a function of β_{xx} and β_{xy} ($x \neq y$), where all values are equal across an interaction type (e.g., $\beta_{xx} := \beta_{bb} = \beta_{cc} = \beta_{ee}$). We observe that the dependence is mostly linear, except that for small values of the inter-species transmission coefficients β_{xy} ($x \neq y$), $\mathcal{R}_0$ is governed entirely by the within-species coefficients β_{xx}. This is not unexpected, but interestingly, the converse is not true: for small values of the within-species transmission coefficients β_{xx}, $\mathcal{R}_0$ remains linearly dependent on β_{xx} and β_{xy}.

4.4. Investigating the effect of competition

Model (2.2) incorporates competition between species. In order to investigate the effect of this competition on the dynamics of the disease, we compare two situations. One is driven by (2.2), the other is similar but has interspecific competition parameters zero, i.e., $d_{xy} = 0$ for $x, y \in \{b, c, e\}$ such that $x \neq y$. In order to have grounds for comparison, for the model without competition, we use for $x \in \{b, c, e\}$, $\tilde{r}_x$, $\tilde{d}_x$ and $\tilde{d}_{xx}$ such that $(\tilde{b}_x - \tilde{d}_x)/\tilde{d}_{xx} = P_x^\star$, i.e., we ensure to compare herds that would have similar sizes at the disease-free equilibrium.

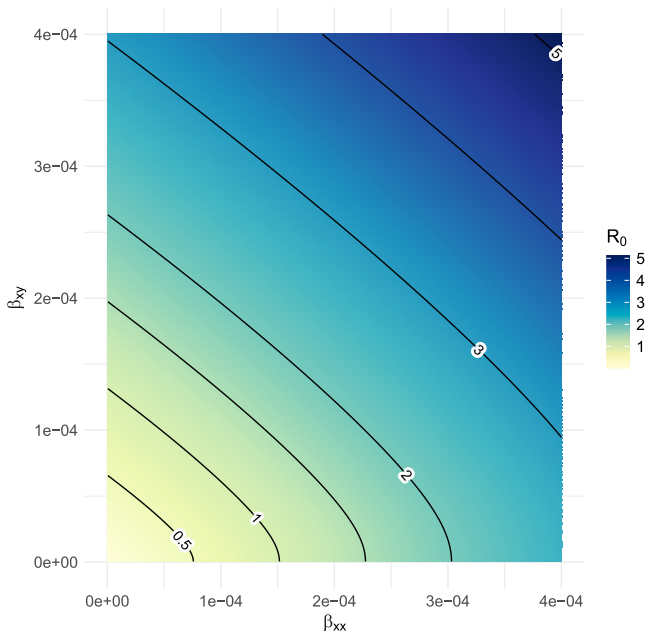

Fig. 3. Value of $\mathcal{R}_0$ as a function of the within-species and between-species transmission coefficients β_{xx} and β_{xy} ($x \neq y$), respectively.

We assume on the other hand that inter-species transmission of the disease occurs. The situation shown there is one where the basic reproduction number for species in isolation is $\mathcal{R}_0^x = 2.5$ for all species. We compute β_{xx} accordingly using (3.11). Regarding between species coefficients β_{xy} ($x \neq y$), we take them to be $0.9\beta_{xx}$, except that $\beta_{be} = 0.7\beta_{bb}$ and $\beta_{eb} = 0.7\beta_{ee}$ to account for potential negative interactions between the larger species. With other parameters as specified in Sections 4.1 and 4.2, the basic reproduction number for the entire system with competition is then $\mathcal{R}_0 \simeq 3.2$.

In Fig. 4, we show solutions for unrealistically long time periods of 200 years to show how competition affects the long term behaviour of the model. We observe in Fig. 4(a) that due to disease-induced death, the resulting total animal population is quite small compared to the disease-free equilibrium value of 560. Extending solutions forward in time using the method in Appendix, we find equilibrium values of roughly 220 and 160 animals in total, with and without competition, respectively. We also observe that the presence of competition hastens convergence to what we suspect is the endemic equilibrium point, with transient oscillations being faster in the system with competition (red curve). Although this has not been proved mathematically, we suspect that the model has a globally asymptotically stable *endemic* equilibrium when $\mathcal{R}_0 > 1$. In the absence of competition, the total population goes to a lower value than when competition is present (when disease is also present).

As with the total animal population, we see in Fig. 4(b) that the presence of competition accelerates convergence of the prevalence of bTB in individual species to an endemic equilibrium (Fig. 4(b) shows bovines, but the same is observed for the other two species). This equilibrium value has fewer infected animals than when competition is present. The same is true for the other two species: the endemic equilibrium with competition has higher prevalence than when competition is absent.

Finally, in Fig. 5, we return to a more realistic time interval of 10 years to focus on the initial response of the model since, in practice, this is the situation that is observed "on the ground". Here, we focus on the difference in prevalence between the case with competition and the case without: when a curve is below zero, prevalence is, at this instant in time, higher for the system without competition than for

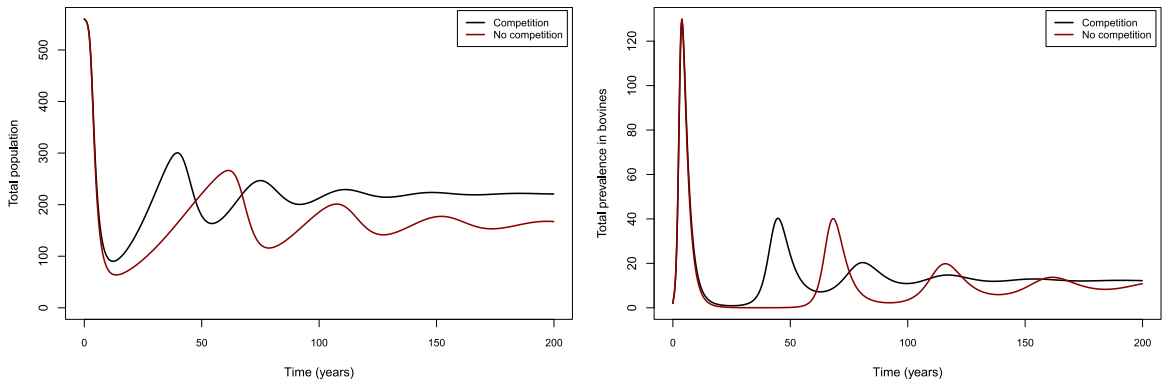

(a) Total animal population (b) Prevalence in bovines

Fig. 4. Comparison of the long term behaviour (200 years) of (2.2) with and without competition. (a) Behaviour of the total animal population $N_b + N_c + N_e$. (b) Prevalence $L_b + I_b$ of bTB in the bovine population.

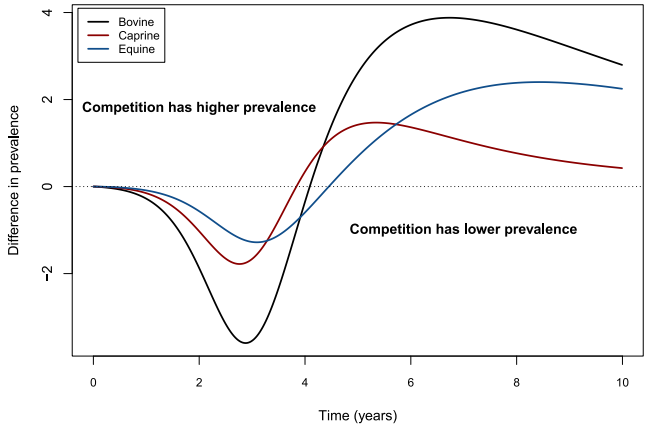

Fig. 5. Difference between total prevalence $L_x(t) + I_x(t)$ with competition present or absent. Below the horizontal axis, prevalence is larger in the absence of competition, above the axis, prevalence is larger when competition is present.

Table 2
Transition rates of the CTMC analogue of competition model (2.1).

Transition	Event, with $x, y \in \{b, c, e\}$	Rate
$N_x \to N_x + 1$	Recruitment of an x	$r_x N_x$
$N_x \to N_x - 1$	Natural death or sale of an x	$d_x N_x$
$N_x \to N_x - 1$	Death x b/c of competition with y	$d_{xy} N_x N_y$

Table 3
Transition rates of the CTMC analogue of epidemiological model (2.2).

Transition	Event, with $x, y \in \{b, c, e\}$	Rate
$S_x \to S_x + 1$	Recruitment of an S_x	$r_x N_x$
$S_x \to S_x - 1$	Natural death or sale of an S_x	$d_x S_x$
$L_x \to L_x - 1$	Natural death or sale of an L_x	$d_x L_x$
$I_x \to I_x - 1$	Natural death or sale of an I_x	$d_x I_x$
$S_x \to S_x - 1$	Death S_x b/c of competition with y	$d_{xy} S_x N_y$
$L_x \to L_x - 1$	Death L_x b/c of competition with y	$d_{xy} L_x N_y$
$I_x \to I_x - 1$	Death I_x b/c of competition with y	$d_{xy} I_x N_y$
$(S_x, L_x) \to (S_x - 1, L_x + 1)$	Infection of an S_x by an I_y	$\beta_{xy} S_x I_y$
$L_x \to L_x - 1$	End of incubation of an L_x	$\epsilon_x L_x$
$I_x \to I_x - 1$	Death of an I_x b/c of bTB	$\delta_x I_x$

the system with competition; when a curve is above zero, the system with competition experiences a higher prevalence. This allows to focus on the part of the curve where solutions appear indistinguishable in Fig. 4(b) (and for the other species). We observe that in the first four or so years of spread, the presence of competition makes the situation "better", then the situation reverses. If one considered longer time intervals, then one would observe several such reversals (e.g., for bovines when the black and red curves intersect in Fig. 4(b)), but as mentioned above, in the limit all curves are above zero, i.e., prevalence is higher when competition is present.

4.5. Stochastic simulations

In order to check that rates found in Section 4.1 are realistic, we consider a continuous-time Markov chain (CTMC) equivalent of (2.1). To better understand how transmission happens between species, we also consider the CTMC equivalent to (2.2). We derive these CTMCs without providing much detail; refer to standard references on conversions between ODE and CTMC, e.g., [38]. Suffices to say here that since rates in (2.1) and (2.2) are constant, the CTMCs corresponding to these systems are homogeneous with transition rates as summarised in Tables 2 and 3.

We start by "validating" the rates found in Section 4.1. Indeed, while the procedure described does produce rates such that (2.1) converges to the desired equilibrium, these rates sometimes lead to very high turnover rates in the species, which we call "fast dynamics" in the sequel.

For instance, consider Fig. 6, which shows (top row) the total head count for the three species and (bottom row) the number of recruitment and removal events taking place in the bovine population (recruitment $r_b N_b$, natural death or sale $d_b N_b$, intra-specific competition $d_{bb} N_b^2$ and inter-specific competition $d_{bc} N_b N^c$ and $d_{be} N_b N_e$) in two sample realisations of the CTMC analogue for competition model (2.1), i.e., considering populations N_b, N_c and N_e with transitions and rates as in Table 2. We show only the bovine population in Figs. 6(c) and 6(d); events for caprines and equines show similar patterns, albeit at slightly slower rates since the populations are smaller.

All figures in Fig. 6 were generated with parameters found using the procedure in Section 4.1. However, only Figs. 6(a) and 6(c) make any sense in terms of the number of recruitment and removal events likely to occur in a herd of the size under consideration. We refer to this regime as "reasonable dynamics", to distinguish it from the "fast dynamics" of Figs. 6(b) and 6(d).

Fig. 6 highlights the consequences of non-identifiability of parameters [39] and the value of CTMCs as a tool to validate the rates found by parameter identification.

We now turn to the CTMC analogue of the full epidemiological model (2.2), with transitions and rates in Table 3. As with the underlying competition model (2.1), the CTMC allows to check that the rates used are consistent. In Fig. 7, we show a sample run over 100

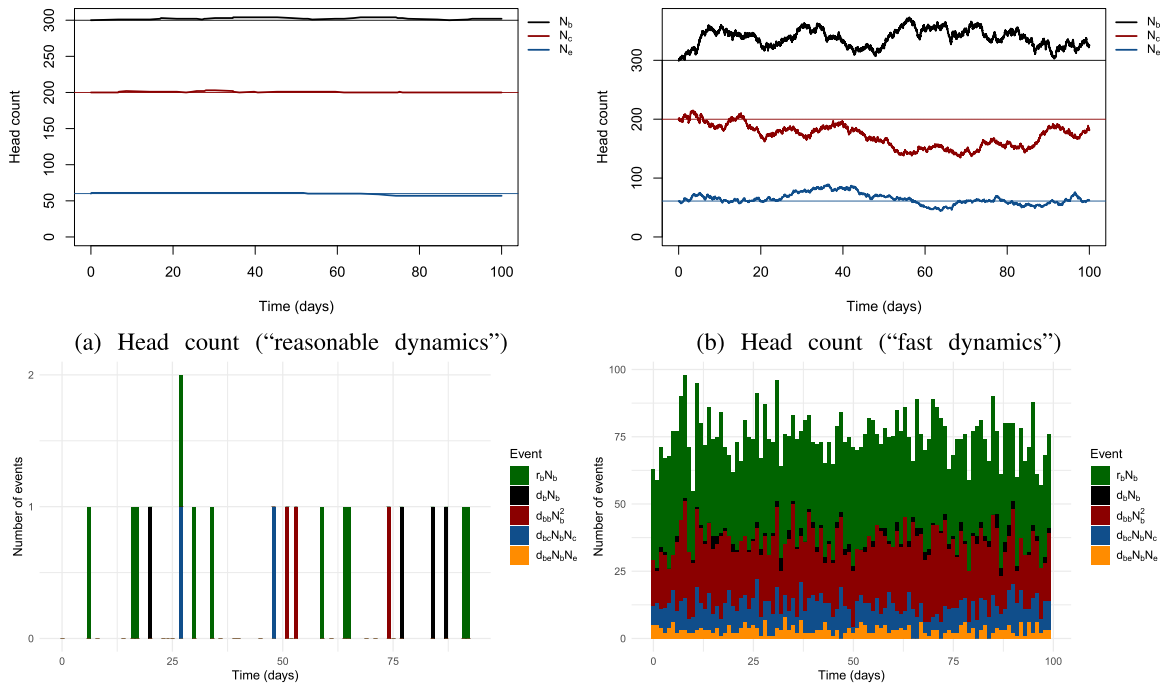

(a) Head count ("reasonable dynamics") (b) Head count ("fast dynamics")

(c) Bovine events ("reasonable dynamics") (d) Bovine events ("fast dynamics")

Fig. 6. Total head count (a,b) and daily number of recruitment and removal events for the bovine population (c,d) in the CTMC analogue of competition model (2.1).

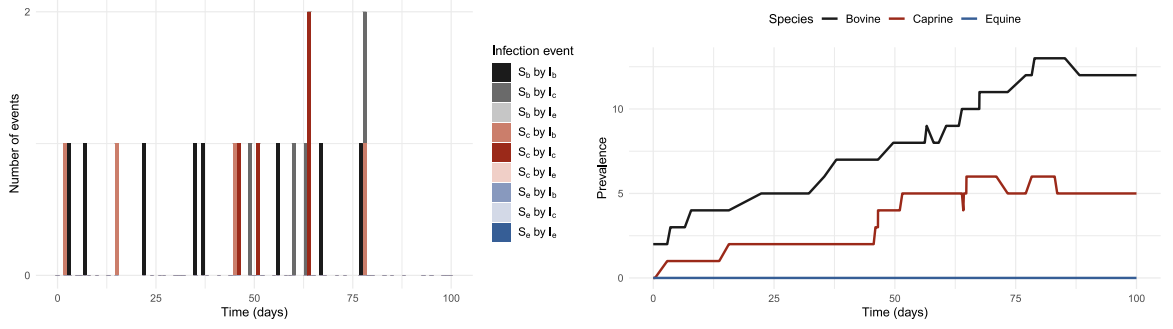

(a) Contamination events (b) Disease prevalence

Fig. 7. (a) Number, timing and nature of the infection events occurring during a sample run of the CTMC analogue of epidemiological model (2.2). (b) Corresponding prevalence $L_x + I_x$ in each of the three species.

days of the model with $\mathcal{R}_0^x = 2.5$ and other parameters as discussed in Sections 4.1 and 4.2. Initial conditions were $L_b(0) = I_b(0) = 1$, with the initial prevalence in the other two species being zero. This particular realisation of the Markov chain illustrates one important difference between the ODE and the CTMC: over the time period considered here, no infection affects equids, whereas with a reproduction number larger than 1, this is not possible for such a duration of time in the ODE.

Moving forward, we now consider large numbers of realisations of the CTMC to investigate some aspects that are complicated to approach using ODEs.

In Fig. 8, we consider the percentage of simulations seeing absorption into the disease-free state as a function of the initial condition and $\mathcal{R}_0$. As the chain has discrete and bounded state space and the disease-free equilibrium is accessible from all states and is the sole absorbing state, the probability of absorption into the DFE is 1 (regardless of the value of $\mathcal{R}_0$), but this may take a *very* long time to happen. So in practice, we restrict ourselves to a time interval that makes sense from an epizootical point of view and compare realisations on this interval.

Initial conditions in Fig. 8 are taken as $L_x = 0$ for all $x \in \{b, c, e\}$ and either $I_b = 1$, $I_c = 1$ or $I_e = 1$ and the two remaining populations starting with no infectious individuals. We observe that at any $\mathcal{R}_0$ value, bovines and caprines, whose populations are larger, see fewer extinction events on average than the smaller equine population. Fig. 8 also illustrates the fundamental difference between ODE and their CTMC analogues: there is non negligible number of realisations of the chain that go extinct when $\mathcal{R}_0 > 1$. Conversely, there are quite a few realisations that see infection persisting for more than 6 months when $\mathcal{R}_0 < 1$. In the latter case, if we were to increase the length of the time interval considered, realisations hovering close to zero prevalence because of a low value of $\mathcal{R}_0$ would increasingly be absorbed. However, the overall shape and ordering of the curves would not change.

Note that the jaggedness of the curves in Fig. 8 results from the number of realisations used to produce each point (20,000 here). When considering, as in Fig. 8, problems related to the probability of disease extinction given an initial number of infectious cases, much finer (and exact) values are obtained using multitype branching process approximations of the continuous time Markov chain. Because this is

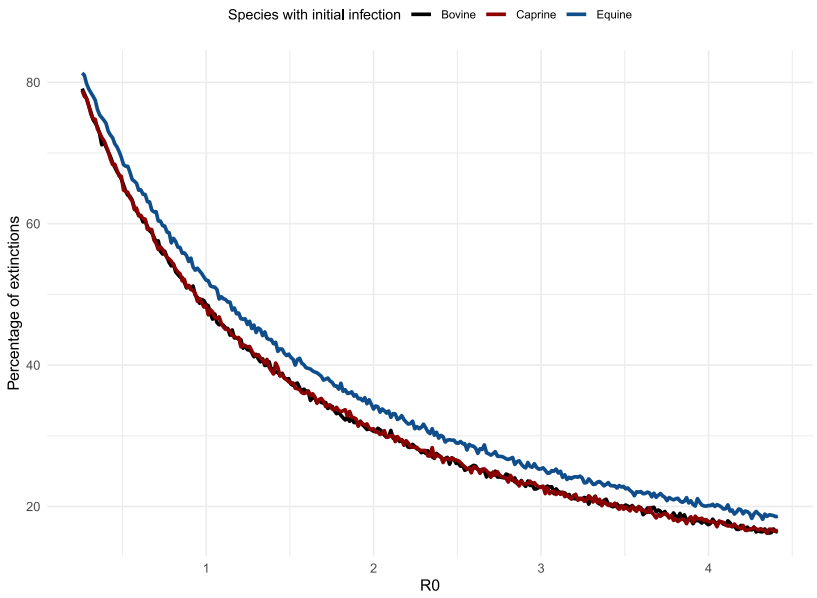

Fig. 8. Percentage of 20,000 simulations seeing disease extinction, as a function of $\mathcal{R}_0$ and depending on which species bears the initial case. The bovine and caprine curves roughly overlap.

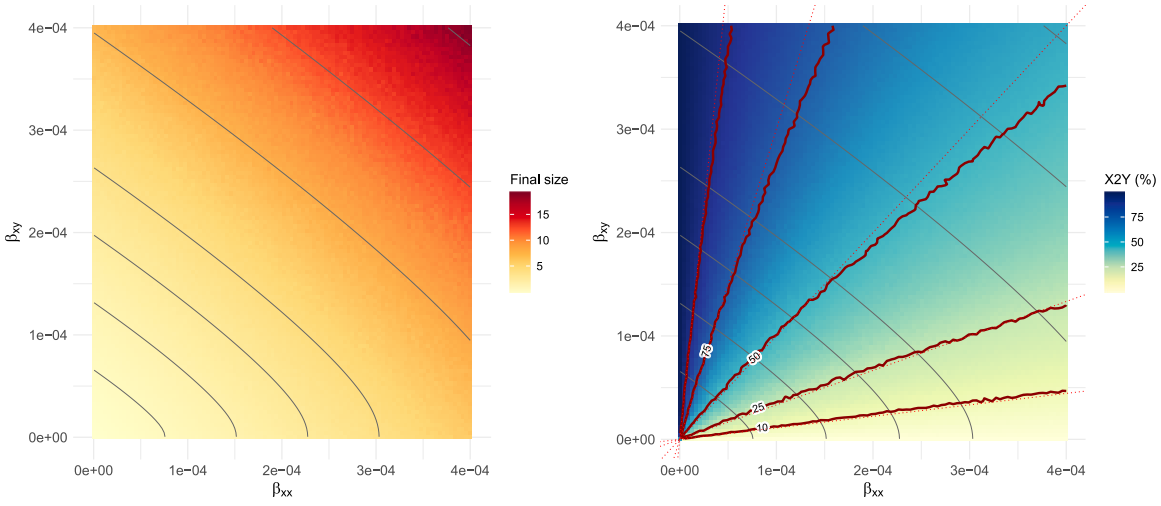

(a) Final size (b) Percentage of $X2Y$ infection

Fig. 9. (a) Heatmap of the number of new cases over a 6 months period. (b) Heatmap of the percentage of these new cases originating from contacts between species ($X2Y$ rather than $X2X$), with 10, 25, 50, 75 and 90-th percentile shown as red curves. Dotted red lines show corresponding percentile area of the first quadrant. (a,b) Grey lines are the level curves of $\mathcal{R}_0$ in Fig. 3.

not the main focus of the paper, we do not follow this approach here and instead settle for irregular curves.

To conclude, we investigate numerically the "final size" (Fig. 9(a)) and the origin of infections (Fig. 9(b)), in the same context as used in Fig. 3, varying the coefficients β_{xx} and β_{xy} of within-species and between-species transmission, respectively, within the same range used there. All other parameters are also taken as in Fig. 3. We show as grey lines the values of $\mathcal{R}_0$ in Fig. 3. Both figures in Fig. 9 are obtained from the same set of simulations, which are conducted as follows: at each point in the $10^2 \times 10^2$ grid sampled, we run 5,000 simulations with initial conditions $I_b(0) = 1$ and all other infected compartments empty. We record the total number of infection events as well as the number of those events originating from contact between individuals of the same species.

Fig. 9(a) shows the final size, i.e., the total number of infections, over the six month period simulations are run for. The final size is normally computed over the duration of an outbreak, which here would involve conditioning on extinction of the chain. However, we do not do so here and count all infections: as far as herders are concerned, whether or not the event is over is irrelevant. In practice, Fig. 9(a) shows that the final size closely aligns with $\mathcal{R}_0$. This is expected, but it is useful to confirm that this is indeed the case: there does not seem to be conditions where reducing the reproduction number would lead to, say, unexpected increases in the burden of infection.

Finally, Fig. 9(b) considers the percentage of between-species ($X2Y$) transmissions in the overall number of transmissions ($X2X$ and $X2Y$). To facilitate interpretation, we show as dotted red lines the lines with slopes β_{xy}/β_{xx} equal to 1/9, 1/3, 1, 3 and 9, corresponding to surface areas of 10%, 25%, 50%, 75% and 90% of the first quadrant, respectively. When the plotted percentage of $X2Y$ infections match these lines, the contribution to $X2Y$ infections observed matches exactly what can be expected from the ratio β_{xy}/β_{xx}. Starting with the 50-th percentile curve

and with higher transmission rates (the fourth from the origin grey line corresponds to $\mathcal{R}_0 = 2$, see Fig. 3), observed percentages of $X2Y$ transmissions are below the corresponding dotted red lines, meaning that it takes smaller values of β_{xy} to achieve a given percentage of $X2Y$ infections: β_{xy} plays a more important role. The difference is not extremely marked, however.

5. Discussion

The model introduced here is a first step towards improving our understanding of the dynamics of pathogens in the context of managed small herds comprising animals from several species. This type of herd is prevalent for nomadic herders in the Sahel region and is therefore extremely important to their livelihood. Building on existing work on the competitive Lotka–Volterra system, we formulated a model for spread of bovine tuberculosis between three species that are in competition but existing, because of human management, at an stable population level equilibrium.

We first considered the mathematical analysis of the model and showed that regarding the disease-free equilibrium, the situation is classic, in the sense that this equilibrium is globally asymptotically stable when the basic reproduction number $\mathcal{R}_0$ is below 1 and unstable otherwise. We did not pursue here the analysis of the endemic case, although numerical investigations confirmed that it too appears classic, with all solutions tending to an unique endemic equilibrium when $\mathcal{R}_0 > 1$.

We then proceeded to a computational analysis of the model. We started by considering an inverse problem to find values of parameters of the underlying competition model so that equilibrium numbers of animals matched the known herd composition. Because (2.1) is not identifiable, we used the continuous time Markov chain analogue to (2.1) to assess the validity of the parameters found. This highlights an interesting use of CTMCs: while it is of course easy to compute, say, $r_b N_b$ to derive the instantaneous rate of recruitment of bovines in (2.1), graphs such as in Fig. 6 make it easier to understand what this rate translates to. (Likewise, Fig. 7(a) is easier for someone with field experience in epizootics to relate to.) We considered the effect of competition on the dynamics of disease spread and observed that when the disease starts to spread in a herd, the presence of competition leads to lower prevalences than are observed when competition is absent. The situation then reverses several times over the course of spread and when the endemic equilibrium is reached, competition always results in a higher prevalence of infection. Finally, we considered the CTMC version of the full epidemiological model to effect the role of the species in which the infection starts as well as the number of animals contaminated and fraction of these contaminations originating from between species contacts. With respect to these aspects, the model behaved very predictably, although the observation that at high reproduction number values, interspecies contamination plays a more important role (Fig. 9(b)) hints that field work would be required to get a better understanding of this parameter.

To conclude, remark that our assumption for considering stable coexistence as the underlying regime of the competition model is that herders are able to replace animals dying because of intra- and interspecific competition as well as because of infection. This is certainly true at the level of a single herd, but if reasoning at a higher geographical level, it may be an issue: if many herds experience the same conditions, e.g., because of a changing climate, then it may become difficult for a herd to be replenished in this way.

CRediT authorship contribution statement

H. Djimramadji: Writing – original draft, Investigation, Formal analysis, Conceptualization. **Julien Arino:** Writing – review & editing, Writing – original draft, Visualization, Validation, Supervision, Project administration, Methodology, Investigation, Formal analysis, Conceptualization. **P.M. Tchepmo Djomegni:** Writing – review & editing, Writing – original draft, Supervision, Methodology, Investigation, Formal analysis, Conceptualization. **M.S. Daoussa Haggar:** Writing – review & editing, Supervision, Methodology, Investigation.

Declaration of competing interest

The authors declare that they have no known competing financial interests or personal relationships that could have appeared to influence the work reported in this paper.

Acknowledgements

The authors thank two anonymous referees whose detailed and thoughtful comments greatly improved the quality of the manuscript. JA is supported in part by an NSERC Discovery Grant .

Appendix. Ensuring convergence of solutions to an equilibrium

In several places, we use the simulation of the ODEs to find the values of endemic equilibria. However, given the wide variety of parameter values considered, there are cases where convergence to these equilibria can be quite slow. For instance, when $\mathcal{R}_0 > 1$ but is very close to 1, if initial conditions are far from the EEP, the system can take a very long time to converge to the EEP.

In order to circumvent this issue while remaining computationally efficient, we use the following procedure, where time units are assumed to be days.

1. Set an individual simulation length ($t_s = 100$ in our code).
2. Set a maximum time for convergence ($t_m = 50{,}000$ in our code).
3. Set a threshold for convergence ($\tau = 10^{-8}$ in our code) and `converged` to FALSE.
4. Set current time $t_c = 0$ and initial conditions $\boldsymbol{x}(t_c) = \boldsymbol{x}_0$.
5. Repeat until `converged` or $t_c \geq t_m$:
   (a) Run the numerical solver with initial condition $\boldsymbol{x}(t_c)$ from $t = t_c$ to $t = t_c + t_s$, using a relatively fine time grid (we use 0.05 days by default).
   (b) Set initial condition as $\boldsymbol{x}(t_c + t_s)$.
   (c) Set $t_c \to t_c + t_s$.
   (d) Compute change in successive solutions. If change is less than τ, set `converged` to TRUE.

To evaluate the change in solutions, we use the last time point $t_f = t_c + t_s$ and the point t_ℓ immediately left of it on the time grid. We then compute the supremum norm

$$\|\boldsymbol{x}(t_f) - \boldsymbol{x}(t_\ell)\|_\infty = \max_{i=1,\ldots,N} \left\{ |x_i(t_f) - x_i(t_\ell)| \right\}.$$

References

[1] D. Njinkeu, F. Tchana Tchana, J.S. Lohi, M.O. Alli, Chad's Livestock: Securing Cross-Border Value-Chain Post-COVID-19, Technical report, The World Bank, 2024.
[2] Bureau du Haut-Commissariat des Nations Unies aux Droits de l'Homme, Le droit à l'alimentation et les conflits agriculteurs-éleveurs au Tchad, 2023.
[3] M. Guindé, O. Ouagal Mahamat, M. Abdallah, Importance du pastoralisme au tchad, Bull. de L' OIE 2 (2018).
[4] D. Keiba, I.R. Muhammed, D. Khassim, G. Yusuf, M. Ousseini, M.I. Abdel-hadi, A.I.I. Dagal, Perception and adaptation of pastoralists in tandjilé-est southern chad to climate change, Niger. J. Anim. Prod. 50 (3) (2023) 72–85.
[5] B.N. Ngandolo, C. Diguimbaye-Djaibé, B. Müller, L. Didi, M. Hilty, I. Schiller, E. Schelling, B. Mobeal, B.S. Toguebaye, A.J. Akakpo, Diagnostics ante et post mortem de la tuberculose bovine au sud du tchad: cas des bovins destinés à l'abattage, Rev. d'élevage médecine vétérinaire Des Pays Trop. 62 (1) (2009) 5–12.

[6] L. Didi, Caractérisation des Mycobacyéries isolées chez l'homme et les ruminants domestiques au Tchad: Causes des suspicions de la tuberculose dans les hôpitaux et aux abattoirs, (Master's thesis), Université Cheikh Anta Diop de Dakar, 2014.
[7] P.B. Phepa, F. Chirove, K.S. Govinder, Modelling the role of multi-transmission routes in the epidemiology of bovine tuberculosis in cattle and buffalo populations, Math. Biosci. 277 (2016) 47–58.
[8] M.D.F. Shirley, S.P. Rushton, G.C. Smith, A.B. South, P.W.W. Lurz, Investigating the spatial dynamics of bovine tuberculosis in badger populations: evaluating an individual-based simulation model, Ecol. Model. 167 (1–2) (2003) 139–157.
[9] C.L. White, S. Harris, Bovine tuberculosis in badger (meles meles) populations in southwest England: an assessment of past, present and possible future control strategies using simulation modelling, Philos. Trans. R. Soc. London [Biol] 349 (1330) (1995) 415–432.
[10] N.D. Barlow, Non-linear transmission and simple models for bovine tuberculosis, J. Anim. Ecol. 69 (4) (2000) 703–713.
[11] E.A.J. Fischer, H.J.W. Van Roermund, L. Hemerik, M.A.P.M. Van Asseldonk, M.C.M. De Jong, Evaluation of surveillance strategies for bovine tuberculosis (mycobacterium bovis) using an individual based epidemiological model, Prev. Vet. Med. 67 (4) (2005) 283–301.
[12] A.M. Perez, M.P. Ward, A. Charmandarián, V. Ritacco, Simulation model of within-herd transmission of bovine tuberculosis in argentine dairy herds, Prev. Vet. Med. 54 (4) (2002) 361–372.
[13] G. Rossi, P. Aubry, C. Dubé, R.L. Smith, The spread of bovine tuberculosis in Canadian shared pastures: Data, model, and simulations, Transbound. Emerg. Dis. 66 (1) (2019) 562–577.
[14] G. Rossi, G.A. De Leo, S. Pongolini, S. Natalini, S. Vincenzi, L. Bolzoni, Epidemiological modelling for the assessment of bovine tuberculosis surveillance in the dairy farm network in Emilia-Romagna (Italy), Epidemics 11 (2015) 62–70.
[15] R.L. Smith, Y.H. Schukken, Z. Lu, R.M. Mitchell, Y.T. Grohn, Development of a model to simulate infection dynamics of mycobacterium bovis in cattle herds in the United States, J. Am. Vet. Med. Assoc. 243 (3) (2013) 411–423.
[16] R.G. Bowers, J. Turner, Community structure and the interplay between interspecific infection and competition, J. Theoret. Biol. 187 (1) (1997) 95–109.
[17] R.K. McCormack, L.J.S. Allen, Disease emergence in multi-host epidemic models, Math. Med. Biol. 24 (1) (2007) 17–34.
[18] K. Mian-Oudanang, S. Pabamé, N. Antoine-Moussiaux, Characterization of pastoral herding in kanem (chad), Int. J. Livest. Prod. 6 (1) (2015) 8–15.
[19] C.J.C. Phillips, C.R.W. Foster, P.A. Morris, R. Teverson, The transmission of mycobacterium bovis infection to cattle, Res. Vet. Sci. 74 (1) (2003) 1–15.
[20] R.M. Almarashi, C.C. McCluskey, The effect of immigration of infectives on disease-free equilibria, J. Math. Biol. 79 (2019) 1015–1028.
[21] T. Duclairoi, Tuberculose bovine, 2018, Journal l'information élevage pour l'AlliancePastorale, www.alliance.elevage.com.
[22] B. Admassu, E. Kebede, A. Shite, Review on bovine tuberculosis, Eur. J. Biol. Sci. 7 (4) (2015) 169–185.
[23] P. van den Driessche, M.L. Zeeman, Three-dimensional competitive Lotka–Volterra systems with no periodic orbits, SIAM J. Appl. Math. 58 (1) (1998) 227–234.
[24] M. Gyllenberg, P. Yan, On a conjecture for three-dimensional competitive Lotka-Volterra systems with a heteroclinic cycle, Differ. Equ. Appl. 1 (2009) 473–490.
[25] M.W. Hirsch, Systems of differential equations which are competitive or cooperative: III. Competing species, Nonlinearity 1 (1) (1988) 51.
[26] M.L. Zeeman, Hopf bifurcations in competitive three-dimensional Lotka–Volterra systems, Dyn. Stab. Syst. 8 (3) (1993) 189–216.
[27] M. Gyllenberg, P. Yan, Four limit cycles for a three-dimensional competitive Lotka–Volterra system with a heteroclinic cycle, Comput. Math. Appl. 58 (4) (2009) 649–669.
[28] D. Xiao, W. Li, Limit cycles for the competitive three dimensional Lotka–Volterra system, J. Differential Equations 164 (1) (2000) 1–15.
[29] P. Yu, M. Han, D. Xiao, Four small limit cycles around a Hopf singular point in 3-dimensional competitive Lotka–Volterra systems, J. Math. Anal. Appl. 436 (1) (2016) 521–555.
[30] P. van den Driessche, J. Watmough, Reproduction numbers and sub-threshold endemic equilibria for compartmental models of disease transmission, Math. Biosci. 180 (1–2) (2002) 29–48.
[31] Z. Shuai, P. van den Driessche, Global stability of infectious disease models using Lyapunov functions, SIAM J. Appl. Math. 73 (4) (2013) 1513–1532.
[32] V. Jean-Richard, L. Crump, D. Moto Daugla, J. Hattendorf, E. Schelling, J. Zinsstag, The use of mobile phones for demographic surveillance of mobile pastoralists and their animals in chad: proof of principle, Glob. Heal. Action 7 (1) (2014) 23209.
[33] P. Sougnabé, P. Grimaud, Emergence des systèmes pastoraux en savane tchadienne: pour quelle intégration territoriale et sociale? Sécheresse 23 (4) (2012) 271–277.
[34] L. Scrucca, On some extensions to GA package: Hybrid optimisation, parallelisation and islands evolution, R J. 9 (1) (2017) 187–206.
[35] F.D. Menzies, S.D. Neill, Cattle-to-cattle transmission of bovine tuberculosis, Vet. J. 160 (2) (2000) 92–106.
[36] A.K. Refaya, G. Bhargavi, N.C. Mathew, A. Rajendran, R. Krishnamoorthy, S. Swaminathan, K. Palaniyandi, A review on bovine tuberculosis in India, Tuberculosis 122 (2020) 101923.
[37] WOAH, Guidelines for the control of *Mycobacterium tuberculosis* complex in livestock – beyond test and slaughter, Technical report, World Organisation for Animal Health, 2024.
[38] L.J.S. Allen, An introduction to stochastic epidemic models, in: Mathematical Epidemiology, Springer, 2008, pp. 81–130.
[39] N. Cunniffe, F. Hamelin, A. Iggidr, A. Rapaport, G. Sallet, Identifiability and Observability in Epidemiological Models, Springer, 2024.